Bombardment of Cadmium Sulfide Crystals with 30- to 60-kev Electrons

C. E. Bleil, D. D. Snyder, and Y. T. Sihvonen
General Motors Research Staff, Detroit, Michigan

(Received May 9, 1958)

The dependence of induced conductivity in CdS crystals on the rate of arrival and the energy of impinging electrons is reported. These results lead to a qualitative picture of the conduction, excitation, and recombination phenomena in CdS which is satisfied by the simple model of a sulfur vacancy, and an analytical expression which involves the mobility of carriers, their effective masses, the number of ground states in the forbidden gap (for pure but not perfect crystals) and their positions as a function of temperature. The red and green luminescence observed under irradiation by electrons is qualitatively explained. The equation for the induced conductivity is derived from the expression for two-carrier conductivity and the definitions of the steady-state Fermi levels for holes and electrons. An empirical fit to the observed data yields $\sigma=e\mu_n N_c \exp(kT\alpha I-E_{fn}^0)/kT$ for $I<I_s$ and $\sigma=e(\mu_n+\mu_p)N_v \exp[kT\beta(I-I_s)-E_{fp}^0]/kT$ for $I>I_s$. The data reported herein were obtained by using monoenergetic bombarding electrons in the range of 30 to 60 kev. An interesting field effect is reported but no clear interpretation is available to the authors. Corroborating data employing ultraviolet irradiation are described.

INTRODUCTION

THE purpose of this paper is to present results of experiments relating the conduction, excitation, and recombination processes in cadmium sulfide to the intensity and energy of monoenergetic bombarding electrons.

This study began as an investigation of the dependence of the conductivity induced in CdS on the energy of the bombarding electrons. The immediate result was the lack of agreement with the conclusions of Ryvkin *et al.*[1] that above 10 kev the conductivity per unit of incident energy flux is constant. A more extended investigation has led to measurements analogous to those reported in the optical range of electromagnetic radiation.[2] The techniques provide a different approach to the study of compound semiconductors such as CdS. In particular, the results of Rose,[3] Klick,[4] Broser and Warminsky,[5] and Kröger[6] will be considered.

EXPERIMENTAL METHOD

The CdS crystals employed in the experiments to be described were grown by a variation of the vaporization-crystallization method described by Czyzak *et al.*[7] In their final prepared condition, they measured up to approximately 5 mm×5 mm with thicknesses ranging up to 3 mm, and had electroplated indium electrodes. Electrical lead wires were fastened to the indium plate with DuPont 5584 silver paint. Spectrographically, the crystals were analyzed to have the impurities shown in Table I. Shown also in Table I are the dark resistivities of several of the crystals.

An electron microscope, RCA model EMB, provided a beam of monoenergetic electrons of energies from 30 to 60 kev in steps of 5 kev. Provisions were available for adjusting the beam intensity. The crystals were held in special fixtures which could be inserted through a port in the projection lens of the microscope. A brass cap with two apertures was fitted over the crystal holder. Through one aperture the total beam current could be measured, while through the other the beam would impinge upon the crystal. In this manner all but the absorbed electrons could be collected by the cap. The CdS crystals were mounted to provide for temperature, optical, and electrical measurements. The vacuum provided for the electron microscope was 10^{-4} mm Hg. The maximum beam current, measured at the sample position, was $\sim 5\times 10^{-9}$ ampere.

Crystal conductances were measured while the beam energy and the beam current were varied. The estimated accuracy of the energy values is $\pm 1\%$ and the estimate of energy spread is 0.1%. The values used for the beam current are arbitrary units proportional to the measured current. For observations of luminescence, the beam was adjusted for maximum current. The only changes made in the beam were made with the focusing controls, except when a decrease in beam current was desired. To observe the effect of an applied field, an external dc voltage source, variable over the range 0–2000 volts, was used. Spectrometer observations of the crystals under electron bombardment were made through the front porthole in the projection lens of the microscope. A Hilger constant-deviation spectrometer with camera attachment was used for the spectrograms.

CATHODOCONDUCTIVITY

The results of measurements of the conductance induced by electron bombardment (cathodoconductivity), as a function of the electron energy, are given in Fig. 1. Except for the value at 30 kev, the increase in conductance with energy is virtually linear. These results, though in a different energy range from that reported by Ryvkin *et al.*,[1] do not agree with their findings. They found that the induced conductivity per unit of energy

[1] S. M. Ryvkin *et al.*, Zhur. Tekh. Fiz. **24**, 961 (1954).
[2] A. Rose, Proc. Inst. Radio Engrs. **43**, 1850 (1955).
[3] A. Rose, Phys. Rev. **97**, 322 (1955).
[4] C. C. Klick, Phys. Rev. **89**, 274 (1953).
[5] I. Broser and R. Warminsky, Ann. Physik **7**, 289 (1950).
[6] F. A. Kröger, Physica **20**, 1149 (1954).
[7] S. J. Czyzak *et al.*, J. Appl. Phys. **23**, 932 (1952).

TABLE I. Spectrographic analyses and some dark resistivities of the crystals used in this study.

Crystal No.	Type	Color	Resistivity (dark) (10^8 ohm cm)	Analysis Mg (%)	Si (%)	Cu (%)	Sb (%)	Al (%)
1	1	Light yellow	...	[a]	...	[a]	...	...
2	2	Dark yellow	7.64	<0.0001	<0.003	<0.001	...	...
3	1	Light yellow	72.6	<0.0007	<0.003	<0.0005	<0.2	...
4	1	Light yellow	No contacts	...	<0.001	...	...	...
5	1	Light yellow	No contacts	<0.0008	...	<0.0003	...	...
6	1	Light yellow	...	<0.0008	...	<0.0003	...	...
7	2	Dark yellow	1.43	<0.0004	...	<0.004	...	<0.003
8	1	Medium yellow	250	<0.0004	...	<0.001	...	<0.001
9	1	Light yellow	67.7	...	<0.001	...	...	...
10	1	Light yellow	3.24	<0.001	<0.003	<0.0003	...	...
11	1	Light yellow	0.86	...	<0.001	<0.0003	...	<0.00005
12	1	Light yellow	6.0	...	<0.001	<0.0005	...	<0.00005
13	2	Amber	No contacts	...	<0.001	<0.001	...	...
14	3	Amber	No contacts	<0.0001	<0.001	<0.0015	...	<0.00005
15	1	Very light yellow	No contacts	...	...	...	...	<0.0005

[a] No analysis. Crystal grown from CdS powder showing these impurities: <0.0003 Mg; <0.003 Cu. From past experience crystals of this type are always at least an order of magnitude purer than the bulk powder from which they are grown.

is independent of the incident beam energy above about 8 kev.

Figure 2 shows a typical curve for the conductance of a CdS crystal as a function of the incident beam current for a beam energy of 50 kev. Carrier yield, defined by Q_e=No. of carriers/No. of absorbed electrons, calculated from our data gives values from $\sim 10^3$ at the lowest incident beam current to $\sim 10^4$ for beam currents above about 1×10^{-9} ampere. Secondary processes are ignored for this calculation, but will be considered in the discussion.

EXCITATION

All of the various types (see Table I) of crystals available were made to emit red and/or green light in the electron beam. It was found that the emitted colors were internally transmitted and at times the whole crystal appeared to glow, which may have been due to this internal transmission and reflection. It was always easier to get crystals to radiate red light (i.e., luminesce with a lower beam intensity) than green. Higher impurity levels apparently depress the luminescence, as observed by Klick.[4]

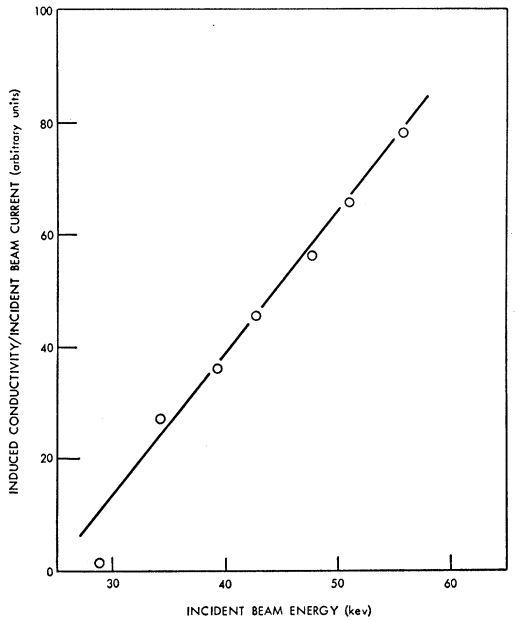

FIG. 1. Conductivity induced in CdS crystal under electron bombardment as a function of electron energy.

The electron beam could be defocused to cover most of the face of a crystal and cause it to luminesce red, but the beam had to be much more concentrated (i.e., of higher local intensity) to cause green luminescence. This relationship always existed regardless of how easy or difficult it was to cause any emission. The beam cross section determined the limit on the size of the colored areas. In our case, the red areas were as large as about 5 mm in diameter and the green areas were about 2 mm maximum diameter.

Using one of the Type 1 crystals, the electron beam was adjusted so that there was only a red spot about 2 mm in diameter. A dc field of about 1000 volts/cm was applied across the crystal. After a few seconds, the red spot was observed to change to green. New apparatus is now being constructed to study this phenomenon further. Tentatively, the field effect might be explained on the assumption of a localized avalanche effect even though the fields were one to two orders of magnitude smaller than is normally required.

The spectral analysis, employing Kodak I-L plates, of the luminescence produced in the crystal while in the electron beam gave a green peak at about 5200 A and a red peak at about 7200 A. These values were corroborated by analysis of crystals irradiated with ultraviolet. If the temperature of the crystal (irradiated by ultraviolet) is reduced by submersion in liquid air, the visible red peak disappears and the green peak breaks up into several peaks, as others have observed.[8–10] If the

[8] R. W. Smith, Phys. Rev. **105**, 900 (1957).
[9] J. Lambe, Phys. Rev. **98**, 985 (1955).
[10] Lambe, Klick, and Dexter, Phys. Rev. **103**, 1715 (1956).

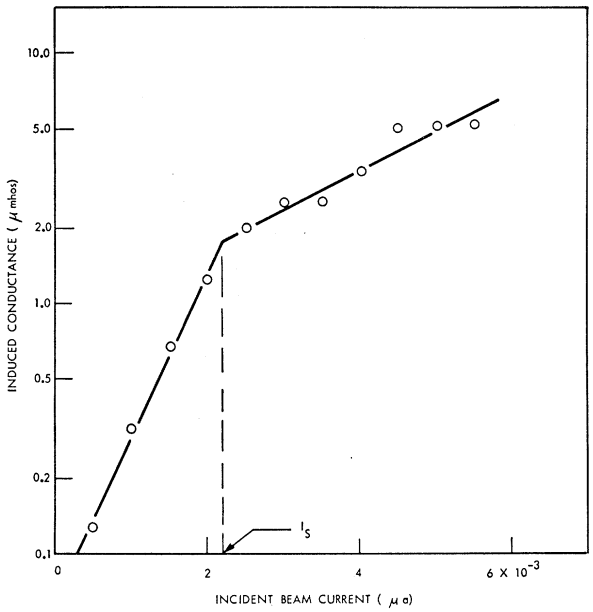

FIG. 2. Conductivity induced in CdS crystal under 50-kev electron bombardment as a function of beam current.

electron beam is caused to impinge on an aluminum target placed near the crystal, the x-rays produced are of sufficient intensity to cause the crystal to luminesce both red and green. We believe that this is the first time luminescence in CdS crystals under x-ray irradiation at room temperature has been reported. Figure 3 shows how the luminescence (both red and green) and the conductivity vary with the intensity of the incident ultraviolet light (qualitative agreement under electron bombardment is observed, but quantitative data are not yet available). It should be noted that the green luminescence is just becoming noticeable at I_s and thus coincides with the break in the conductivity curve.

DISCUSSION

Several models have been proposed to explain the interesting characteristics of cadmium sulfide. For example, it has been suggested that sulfur vacancies could satisfy the requirements of Kröger's[6] exciton model for the interpretation of the green edge luminescence observed at 77°K. Lambe[9] suggests that the exciton model is not valid on evidence obtained at 4°K, but retains the model of the sulfur vacancy to explain green edge luminescence at low temperature. Rose[3] generally describes the photoconductive processes on the basis of two classes of states within the forbidden gap. Bube[11] suggests that sulfur and cadmium vacancies satisfy the requirements of the two classes proposed by Rose. On the assumption of Rose's model explanations for nonlinear photocurrent-light curves, infrared quenching, thermally stimulated currents, and some other related phenomena are claimed. The model proposed in this paper is in general agreement with those proposed above with a few exceptions.

It is proposed that in very pure CdS crystals sulfur vacancies account for most of the phenomena observed. Specifically, transitions *to* energy levels in the forbidden gap involving non-ionized and singly ionized final states or transitions *from* energy levels in the forbidden gap involving nonionized or singly ionized initial states provide the necessary recombination rates to postulate two classes of states in the gap.[2,7] In particular, the recombination centers are classified as follows:

Class I = ionized center;

Class II = non-ionized center.

However, the numbers of occupied states of the two classes respectively are not unrelated on the basis of the above assumption. In fact, it is because of the relationship of the population of the two classes of states that the following description of the results reported in this paper can be made.

The particular crystal arrangement used to obtain the data given in Fig. 2 was a thin (~250 micron) CdS crystal with indium electroplated on one side and an approximately 100-angstrom layer of copper sputtered on the other side. The copper side was placed toward the electron beam. The beam itself was less than 50 microns in diameter and since the depth of penetration of 50-kev electrons is of the order of 10 microns, it is believed that secondary processes involving electromagnetic radiation are responsible for creation of free carriers throughout

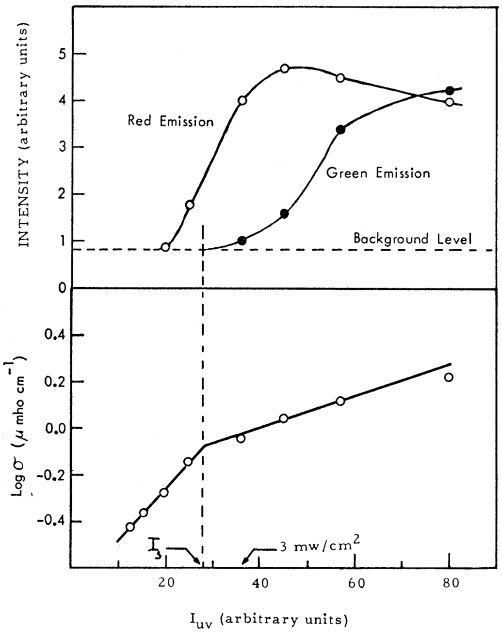

FIG. 3. Luminescence and conductivity of a Type 1 CdS crystal as a function of the intensity of irradiating ultraviolet light. The drooping of the luminescence curves at high intensity is considered due to temperature increase in the crystal. [Figure after A. Vuylsteke and Y. T. Sihvonen (to be published).]

[11] R. H. Bube, Proc. Inst. Radio Engrs. 43, 1836 (1955).

the crystal. The production of visible green and red luminescence throughout the crystal is not a necessary consequence of these secondary processes. In fact, it is probable that only in the immediate vicinity of the electron beam is the carrier density sufficiently high to give appreciable visible luminescence. This effect would mask lesser amounts of luminescence from other areas, particularly when internal reflection occurs.

For the development that follows, it will be assumed that the entire crystal participates homogeneously in the conductivity. This assumption may not be entirely correct for the case of the electron beam; nevertheless, the following development fits the gross response of the CdS crystal in an electron beam and should apply even better to more extended sources.

From these experiments (Fig. 3) it is observed that the cathodoconductivity σ is a function of the bombarding beam current. The conductivity for a semiconductor is given by

$$\sigma = ne\mu_n + pe\mu_p, \tag{1}$$

where n and p are the carrier densities and μ_n and μ_p are their respective mobilities. The steady-state Fermi levels (SSFL) for electrons and holes are defined by

$$n = N_c \exp(-E_{fn}/kT), \tag{2}$$

$$p = N_v \exp(-E_{fp}/kT), \tag{3}$$

where N_c and N_v are the number of effective states/cm^3 in the conduction and valance band, respectively, E_{fn} is the energy separation of the conduction band and the SSFL for electrons, and E_{fp} is the energy separation of the valence band and the SSFL for holes. Differentiating Eqs. (1), (2), and (3) and combining, we have

$$\begin{aligned} d\sigma/dI = {} & e(\partial\mu_n/\partial I)N_c \exp(-E_{fn}/kT) \\ & -(e\mu_n N_c/kT)(\partial E_{fn}/\partial I)\exp(-E_{fn}/kT) \\ & +e(\partial\mu_p/\partial I)N_v \exp(-E_{fp}/kT) \\ & -(e\mu_p Nv/kT)(\partial E_{fp}/\partial I)\exp(-E_{fp}/kT). \end{aligned} \tag{4}$$

If one assumes that the curve of σ *versus* I corresponds to increasing occupancy of the recombination centers until at S in Figs. 2 and 3 these centers become saturated, then, beyond S, a second recombination accounts for the change in properties of the crystal. This corresponds to a gradual raising of the SSFL for electrons accompanied by very little movement of the SSFL for holes until the ground states within the band gap become saturated.

Above saturation free holes play a significantly more important role in the response of the semiconductor since the rate of free hole generation equals the rate of free electron generation. Furthermore, since below saturation the holes generated are trapped almost immediately, their mobility and $(\partial\mu_p/\partial I)$ are negligibly small. Above saturation, however, the mobility for electrons has reached a maximum and $(\partial\mu_n/\partial I)\approx 0$ whereas μ_p and $(\partial\mu_p/\partial I)$ cannot now be neglected. The above results are expressed as

$$(\partial E_{fp}/\partial I)\approx 0, \quad (\partial\mu_p/\partial I)\approx 0, \quad \text{for} \quad I<I_S, \tag{5}$$

and

$$(\partial n/\partial I)=(\partial p/\partial I), \quad (\partial\mu_n/\partial I)\approx 0, \quad \text{for} \quad I>I_S. \tag{6}$$

Therefore, for the first branch of the curve in Fig. 2 ($I<I_S$) the conductivity becomes

$$\begin{aligned} \sigma_l = \int_0^I & [e(\partial\mu_n/\partial I)N_c \exp(-E_{fn}/kT) \\ & -(e\mu_n N_c/kT)(\partial E_{fn}/\partial I)\exp(-E_{fn}/kT)]dI, \end{aligned} \tag{7a}$$

$$\sigma_l = e\mu_n N_c \exp[-(E_{fn}{}^0 - kT\alpha I)/kT], \tag{7b}$$

where

$$E_{fn} = E_{fn}{}^0 - kT\alpha I. \tag{8}$$

Equation (8) is the empirical relationship satisfying the theoretical results for $I<I_S$. If one now applies Eq. (6) to Eq. (4), the conductivity for $I>I_s$ becomes

$$\begin{aligned} \sigma_h = \int_{I_s}^I & [e(\partial\mu_p/\partial I)N_v \exp(-E_{fn}/kT) \\ & -e(\mu_n+\mu_p)N_v/kT(\partial E_{fp}/\partial I) \\ & \times\exp(-E_{fp}/kT)]dI \end{aligned} \tag{9a}$$

$$= e(\mu_n+\mu_p)N_v \exp\{-[E_{fp}{}^0 - kT\beta(I-I_S)]/kT\}, \tag{9b}$$

where

$$E_{fp} = E_{fp}{}^0 - kT\beta(I-I_S). \tag{10}$$

Here again Eq. (10) is the empirical relationship satisfying the theoretical results for $I>I_S$.

The solid lines in Fig. 2 show the fit to the experimental data. The values of the parameters are

$$\begin{aligned} & \alpha = 1.45\times 10^9 \text{ amp}^{-1}; \\ & \sigma_0 = e\mu_n N_c \exp(-E_{fn}{}^0/kT) = 7.2\times 10^{-8} \text{ mho}, \\ & \beta = 0.36\times 10^9 \text{ amp}^{-1}; \\ & \sigma_s = e(\mu_n+\mu_p)N_v \exp(-E_{fp}{}^0/kT) = 2.0\times 10^{-6} \text{ mho}. \end{aligned} \tag{11}$$

Equating the conductivities at saturation and assuming the mobilities of holes and electrons to be nearly equal, the number of recombination centers is found to be $\sim 10^{10}$/cm^3. A different calculation, which assumes only the visibly green area to five microns depth to be saturated by the entire electron beam, yields a recombination-center density of $\sim 10^{15}$/cm^3. These values reasonably represent the limits of recombination-center density for these crystals.

Equations (8) and (10) of the above development

imply that the net rate of production of the carriers ($n=f\tau$), by whatever primary and secondary processes are involved, depends on the number of carriers already present. The above experiments do not, however, distinguish the dependence of the excitation rate f from that of the lifetime τ on the intensity of radiation.

ACKNOWLEDGMENTS

The authors wish to express their appreciation to Dr. G. M. Rassweiler, Mr. D. R. Boyd, and Dr. R. N. Hollyer, Jr., for stimulating and critical discussions and to Mr. C. D. Woelke for growing and preparing the CdS crystals to our specifications.

PHYSICAL REVIEW VOLUME 111, NUMBER 6 SEPTEMBER 15, 1958

Paramagnetic Resonance Spectrum of Gadolinium in Hydrated Lanthanum Trichloride*

M. WEGER AND W. LOW
Department of Physics, The Hebrew University, Jerusalem, Israel
(Received May 15, 1958)

The paramagnetic resonance spectrum of Gd^{3+} in $LaCl_3\cdot 7H_2O$ was measured and found to agree quite well with a spin Hamiltonian with dominant coefficients $b_2^0=\pm 0.0131$ cm^{-1}, $b_2^2=\mp 0.0075$ cm^{-1} at room temperature, and $b_2^0=\pm 0.0099$ cm^{-1}, $b_2^2=\mp 0.0115$ cm^{-1} at liquid air temperature.

1. INTRODUCTION

THE paramagnetic resonance spectrum of Gd^{3+} in $LaCl_3\cdot 7H_2O$ was investigated in the hope that this substance might be suitable for a maser operation. The long relaxation time of the Gd^{3+} ion and its estimated zero-field splitting (0.1—0.3 cm^{-1}) appeared promising. These estimates seem to have been confirmed by experiment.

There has been considerable work on the absorption spectra of the hydrated rare earth ions including those of gadolinium.[1] It was hoped that these results might be of some help in interpreting the optical spectra. Moreover, gadolinium seemed to be a logical starting point for the investigation of other chlorides of this series having similar crystal structures.

2. CRYSTALLOGRAPHY AND EXPERIMENTAL TECHNIQUE

(a) $LaCl_3\cdot 7H_2O$ is a triclinic crystal for which no crystallographic data seem to be available. Since the crystal has no magnetic axis of symmetry, the determination of its magnetic axes is somewhat more involved than in the trigonal and hexagonal crystals so far investigated. The directions of all the magnetic axes must be determined from the resonance spectrum. The method used here is as follows. The crystal is rotated independently around two nonparallel axes and the direction of maximum splitting of the resonance spectrum is determined. (This direction will be called henceforth the z axis.) The crystal is then rotated in a plane perpendicular to the z axis and the positions of maximum and minimum splitting in this plane are measured (henceforth called x and y axes, respectively). These axes are found to be mutually orthogonal, as expected.

(b) A conventional 3-cm microwave spectrometer is used. One of the two axes of rotation mentioned above is furnished by the magnet which can be rotated in a horizontal plane. The second axis is obtained from a crystal mount in the cavity which can be rotated in a vertical plane (see Fig. 1). To avoid diminution of line strength due to nonorthogonality of the steady magnetic field H_0 and the rf magnetic field, the crystal is mounted in the cavity at a point where the rf magnetic field is vertical. The crystal mount is rotated by an aluminium disk graduated in degrees. The disk is detachable to facilitate work at liquid air temperatures. Accurate alignment of the disk is ensured by a pin and hole arrangement. Backlash is about 3°.

RESULTS AND INTERPRETATION

At room temperature, at a frequency of 9373 Mc/sec, absorption lines were found at the following magnetic fields (in gauss):

913	1607	3097
1789	2181	3157
2618	2738	3339
z axis 3433	x axis 3329	y axis 3667
4246	3991	4200
5082	4728	(three coinciding
6034	5514	lines)

The widths of the lines were of the order of 20–30 gauss.

The spin Hamiltonian which has been applied to this spectrum is

* Supported by the U. S. Air Force, Office of Scientific Research, Air Research Development Command.
[1] G. H. Dieke and L. Leopold, J. Opt. Soc. Am. **47**, 944 (1957).